

Triplet superconductivity in a one-dimensional ferromagnetic $t - J$ model

G.I. Japaridze¹ and E. Müller-Hartmann
*Institut für theoretische Physik,
Universität Köln, 50937 Köln, Germany*

In this paper we study the ground state phase diagram of a one-dimensional $t - U - J$ model, at half-filling. In the large-bandwidth limit and for ferromagnetic exchange with easy-plane anisotropy, a phase with gapless charge and massive spin excitations, characterized by the coexistence of triplet superconducting (TS) and spin density wave (SDW^z) instabilities is realized in the ground state. With reduction of the bandwidth, a transition into an insulating phase showing properties of the spin- $\frac{1}{2}$ XY model takes place. In the case of weakly anisotropic antiferromagnetic exchange the system shows a long range dimerized (Peierls) ordering in the ground state. The complete weak-coupling phase diagram of the model, including effects of the on-site Hubbard interaction, is obtained.

PACS numbers: 71.27.+a, 71.10.Hf, 71.10.Fd

I. INTRODUCTION

Soon after the discovery of superconductivity in copper-oxide systems, a new oxide-superconductor, Sr_2RuO_4 , was discovered [1]. Having the same layered perovskite structure as La_2CuO_4 the layered ruthenate shows a rather unconventional superconducting phase [2–4]. Shortly after the discovery of Sr_2RuO_4 it was suggested that a triplet superconducting phase is realized in this compound [5–7]. Since then convincing experimental evidence has been collected that Sr_2RuO_4 is most likely a p -wave superconductor (for a recent review see [8]). An important feature of related ruthenate compounds is close proximity to magnetic instability ($SrRuO_3$ and Sr_2RuYO_6 are ferro- and antiferromagnetic, respectively), indicating strong correlations in the Ru ions. The NMR studies clearly show tendency towards ferromagnetism in Sr_2RuO_4 [9]. Moreover, very recent experiments indicate the easy-plane anisotropy of ferromagnetic spin fluctuations in this compound [10]. The presence of ferromagnetism in $SrRuO_3$ and the analogy with 3He made Sigrist and Rice predict the triplet nature of superconductivity in Sr_2RuO_4 [5]. Close proximity of the ferromagnetic and triplet superconducting instabilities in Sr_2RuO_4 increase the interest in models providing a mechanism for Cooper pairing via ferromagnetic spin fluctuations [5,11,8].

Another group of unconventional superconductors showing close proximity of magnetic and superconducting ordering belongs to the $(TMTSF)_2X$ family of quasi-one-dimensional conductors (the Bechgaard salts) [12]. At ambient pressure, most of these compounds show a spin-density wave (SDW) ordering in the ground state. Under moderate pressure, the SDW instability is suppressed and replaced by a superconducting transition at a critical temperature of the order of 1 K [13]. The most interesting exceptions to this scheme are: 1) $(TMTSF)_2ClO_4$ which is superconducting at ambient pressure and 2) $(TMTSF)_2PF_6$ which shows a spin-Peierls (SP) phase in the ground state at atmospheric

pressure. In this latter case, increasing pressure leads first to a transition from the SP phase into a SDW phase, and finally to the suppression of the SDW ground state in favor of superconductivity [13]. Triplet superconducting ordering in Bechgaard salts was suggested soon after the discovery of $TMTSF$ systems [14] to explain the strong suppression of T_c by nonmagnetic impurities [15]. Although the symmetry of the superconducting phase in Bechgaard salts still remains the subject of some controversy, growing experimental evidence has been collected in the last few years, indicating that the Bechgaard salts $(TMTSF)_2ClO_4$ and $(TMTSF)_2PF_6$ under pressure are triplet superconductors (TS) [16].

In this paper we put forward a rather simple extension of the Hubbard model by incorporating direct anisotropic exchange (of either sign) between electrons on nearest-neighbor sites. In 1D the Hamiltonian reads:

$$\begin{aligned} \mathcal{H} = & -t \sum_{n,\alpha} (c_{n,\alpha}^\dagger c_{n+1,\alpha} + c_{n+1,\alpha}^\dagger c_{n,\alpha}) \\ & + U \sum_n c_{n,\uparrow}^\dagger c_{n,\uparrow} c_{n,\downarrow}^\dagger c_{n,\downarrow} \\ & + \sum_n \left\{ \frac{1}{2} J_\perp (S_n^+ S_{n+1}^- + h.c.) + J_\parallel S_n^z S_{n+1}^z \right\} \end{aligned} \quad (1)$$

Here $c_{n,\alpha}^\dagger$ ($c_{n,\alpha}$) is the creation (annihilation) operator for an electron at site n with spin α , $\vec{S}(n) = \frac{1}{2} c_{n,\alpha}^\dagger \vec{\sigma}_{\alpha\beta} c_{n,\beta}$ where σ^i ($i = x, y, z$) are the Pauli matrices.

The model (1) was intensively studied in the context of High- T_c superconductivity for strong on-site repulsion and for isotropic antiferromagnetic exchange [17–20]. Below we study the weak-coupling phase diagram of the model (1) focusing on effects of exchange anisotropy, in particular in the case of ferromagnetic exchange. We will show that the one-dimensional version of this (1) model has a ground state phase diagram characterized by the close proximity of *triplet superconducting*, *spin density wave*, *ferromagnetic* and *Peierls dimerized* phases.

That the TS phase can be realized in 1D correlated

electron systems is well known from standard “*g-ology*” studies [21]. The extended (U - V) Hubbard model with nearest-neighbor attraction ($V < 0$) has been intensively studied to explain the competition between SDW and superconducting instabilities in $TMTSF$ compounds [22]. However, due to spin rotational invariance, in the extended Hubbard model the TS phase is realized only in the Luttinger liquid phase for $|U| < -2V$ [21,23,24], where both charge and spin excitations are gapless. Singlet superconducting (SS) and TS correlations show identical power-law decay at large distances and the TS instability dominates only due to weak logarithmic corrections [24]. On the other hand, in the spin gapped phase $U < 2V$, the dynamical generation of a spin gap leads to the *complete suppression* of the TS and SDW instabilities.

In this paper we study the weak-coupling ground state phase diagram of the model (1) at half-filling. As we will show below, in the case of *ferromagnetic easy-plane anisotropy* ($J_{\perp} < J_{\parallel} < 0$), the TS and SDW are the only instabilities in the system. In some sense, the *ferromagnetic $t - J$* model (1) shows infrared behavior which is dual to that of the attractive $U - V$ Hubbard model. This duality is most easily seen by comparing the attractive Hubbard model ($U < 0, J_{\parallel} = J_{\perp} = 0$) and the *ferromagnetic itinerant XY* model ($J_{\perp} < 0, U = J_{\parallel} = 0$). In both models the spin excitation spectrum is gapped and the charge excitation spectrum is gapless. In the attractive Hubbard model the dynamical generation of the spin gap is associated with the suppression of SDW and TS fluctuations. In the ground state only the charge density wave (CDW) and SS correlations survive. At half-filling, due to $SU(2)$ -symmetry of the charge channel, the ground state is characterized by the coexistence of CDW and SS instabilities. Away from half-filling the singlet superconducting instability dominates [25]. In the (weak-coupling limit of the) ferromagnetic itinerant XY model, however, due to the $U(1)$ -spin symmetry, the dynamical generation of a spin gap leads to *complete suppression* of the SS and CDW fluctuations. At half-filling, due to the $SU(2)$ -symmetry of the charge channel, the TS and SDW instabilities coexist (see Fig. 1). Doping of the system, as in the case of the Hubbard model, splits the degeneracy, in this case in favor of the TS ordering.

The Ising part of the ferromagnetic exchange tends to reduce the TS ordering. The line $J_{\parallel} = J_{\perp} = J < 0$, corresponding to *isotropic ferromagnetic exchange* marks the transition into a regime with gapless spin excitations. At half-filling, in the case of isotropic exchange the model (1) is characterized by the high $SU(2) \otimes SU(2)$ symmetry. Due to this symmetry the ground state of the ferromagnetic itinerant XXX model is a Luttinger liquid (LL) phase, characterized by an identical power-law decay of all correlations at large distances. In the case of *ferromagnetic easy-axis* anisotropy ($J_{\parallel} < J_{\perp} < 0$) a LL phase with weakly dominating easy-plane magnetic instabilities is realized. In the case of antiferromagnetic exchange, the line $J_{\perp} = -\frac{1}{2}J_{\parallel}$ marks the transition into a regime

where a charge gap opens. Therefore in the case of *antiferromagnetic easy-axis* anisotropy ($J_{\parallel} > 2|J_{\perp}|$) both the charge and the spin channels are massive and long range SDW^z (Néel) ordering takes place.

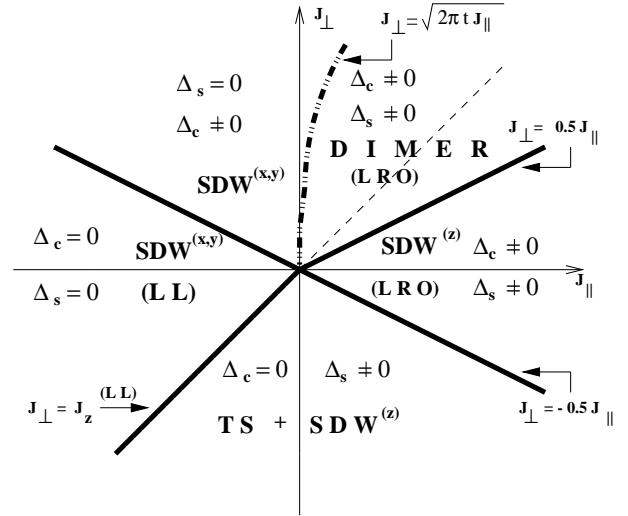


FIG. 1. The weak-coupling phase diagram of the model (1) in the case of a half-filled band and at $U = 0$. $\Delta_{c(s)}$ denotes the charge (spin) gap. Thick lines separate different phases: 1. *Dimer* (LRO) - long range ordered dimerized (Peierls) phase. 2. SDW^z (LRO) - the long range ordered antiferromagnetic (Néel) phase. 3. $SDW^{x,y}$ - insulating state with dominating easy-plane antiferromagnetic correlations. 4. $SDW^{x,y}$ (LL) - Luttinger liquid phase with dominating easy-plane antiferromagnetic correlations. 5. $TS + SDW^z$ - phase with gapless charge and gapped spin excitation spectrum characterized by the coexistence of the triplet superconducting and antiferromagnetic instabilities.

Very rich is the phase diagram of the model (1) in the case of *antiferromagnetic* exchange. The line $J_{\perp} = \frac{1}{2}J_{\parallel} > 0$ is the transition line from the LRO SDW^z phase into a LRO dimerized (Peierls) phase. The long range ordered dimerized phase is realized in particular in the ground state of the antiferromagnetic itinerant XXX model ($J_{\parallel} = J_{\perp} > 0$). The line $J_{\perp} = \sqrt{2\pi t} J_{\parallel}$ marks the transition into an insulating phase with gapless spin excitation spectrum and dominating in-plane (XY) magnetic correlations.

We have to stress the weak-coupling nature of the presented phase diagram. Higher order corrections will modify the shape of borderlines between phases. However, far more important are strong coupling effect. In the case of strong exchange interaction, there are additional phase transitions due to the finite band width. Usually such effects can not be traced within the continuum-limit (infinite band) approach used in this paper and will require numerical studies. Below we focus only on the TS part of the phase diagram and present a qualitative analysis of the transition from the TS phase into a magnetic insulating phase.

Let us first consider the itinerant XY model ($J_{\parallel} = U = 0$). In the weak-coupling limit $|J_{\perp}| \ll t$, the charge excitation spectrum is gapless and the spin excitation spectrum is massive. However, in the limit of strong ferromagnetic exchange $|J_{\perp}| \gg t$, the model is equivalent to the XY spin chain. Therefore, with increasing coupling one has to expect a transition from the regime with massive spin and massless charge excitation spectrum into a insulating magnetic phase with gapless spin excitations. Our finite system studies show (see Fig. 2) that this transition takes place at $J_{\perp}^c \sim -4t$ and is of level crossing type [26]. After the transition the ground state energy of the itinerant model becomes very close to the ground state of the spin- $\frac{1}{2}$ XY chain. In the case of antiferromagnetic exchange there is no transition with increasing $J_{\perp} > 0$ and the system continuously approaches its limiting behavior at $J_{\perp}/t \rightarrow \infty$.

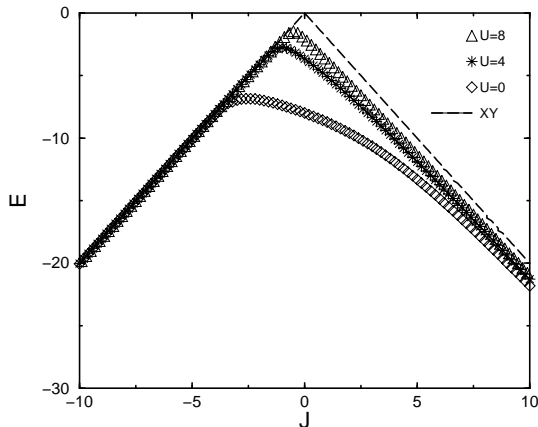


FIG. 2. The ground state energy of the half-filled itinerant XY -Hubbard chain (6 sites) vs. exchange for $U = 0$ (diamonds), $U = 4$ (stars) and $U = 8$ (triangles). The dashed line correspond to the ground state energy of the spin- $\frac{1}{2}$ XY model.

The numerical data presented in Fig. 2 clearly indicate the renormalization of the critical value of the transverse exchange J_{\perp}^c by the on-site Hubbard interaction. In the limit of strong Hubbard repulsion J_{\perp}^c is reduced to values of the order t^2/U . Detailed numerical studies of the strong-coupling phase diagram of the model (1) is in progress and will be published elsewhere.

Figure 3 shows phase diagram of the itinerant- XY -Hubbard model.

Below we will focus on the ferromagnetic part of the phase diagram. We will see that for moderate values of the Hubbard repulsion the TS and the SDW phases survive. In the case of weak exchange one obtains that a charge gap opens at $U > -J_{\perp}$ and a transition into a long range ordered SDW^z phase takes place. Therefore, at $U > 0$ with increasing exchange one has to expect

two different transitions: for $U < |J_{\perp}| < t$ the transition discussed above will take place, but for $U \gg t, |J_{\perp}|$ a “spin-flop” transition from the LRO SDW^z phase into the XY phase has to occur.

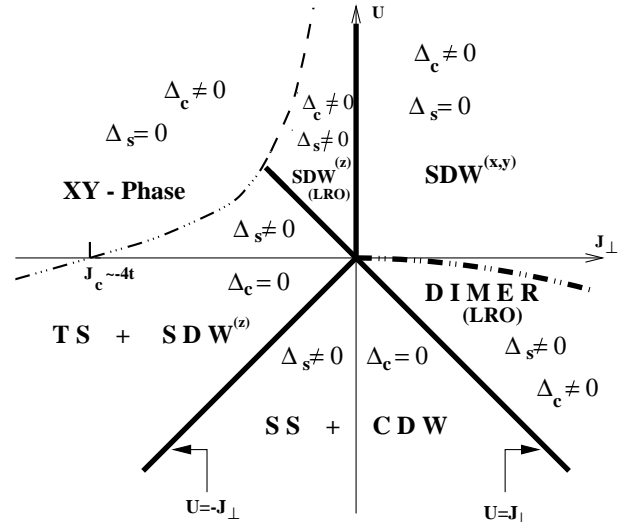


FIG. 3. The weak-coupling phase diagram of the model (1) at $J_{\parallel} = 0$. Solid lines indicate borders between the weak-coupling limit phases. The dashed line marks (qualitatively) the transition into the XY magnetic phase.

The paper is organized as follows: in the next section the weak-coupling continuum-limit version of the model (1) is constructed and the renormalization-group analysis is performed. In the Sect. III, the weak-coupling phase diagram is discussed. Finally, Sect. IV is devoted to a discussion and to concluding remarks.

II. CONTINUUM-LIMIT THEORY AND BOSONIZATION.

In this section we construct the continuum-limit version of the model Eq. (1) at half-filling. While this procedure has a long history and is reviewed in many places [28], for clarity we briefly sketch the most important points.

The field theory treatment of 1D systems of correlated electrons is based on the weak-coupling approach $|U|, |J_{\perp}|, |J_{\parallel}| \ll t$. Assuming that the low energy physics is controlled by states near the Fermi points $\pm k_F$ ($k_F = \pi/2a_0$, where a_0 is the lattice spacing) we linearize the spectrum around these points and obtain two species (for each spin projection α) of fermions, $R_{\alpha}(n)$ and $L_{\alpha}(n)$, which describe excitations with dispersion relations $E = \pm v_F p$. Here, $v_F = 2ta_0$ is the Fermi velocity and the momentum p is measured from the two Fermi points. More explicitly, one decomposes the momentum expansion for the initial lattice operators into two parts centered around $\pm k_F$ to obtain the mapping:

$$c_{n,\alpha} \rightarrow i^n R_\alpha(n) + (-i)^n L_\alpha(n), \quad (2)$$

where the fields $R_\alpha(n)$ and $L_\alpha(n)$ describe right-moving and left-moving particles, respectively, and are assumed to be smooth on the scale of the lattice spacing. This allows us to introduce the continuum fields $R_\alpha(x)$ and $L_\alpha(x)$ by

$$\begin{aligned} R_\alpha(n) &\rightarrow \sqrt{a_0} R_\alpha(x = na_0), \\ L_\alpha(n) &\rightarrow \sqrt{a_0} L_\alpha(x = na_0). \end{aligned} \quad (3)$$

In terms of the continuum fields the free Hamiltonian reads:

$$\mathcal{H}_0 = E_0 - iv_F \sum_\alpha \int dx [: R_\alpha^\dagger \partial_x R_\alpha : - : L_\alpha^\dagger \partial_x L_\alpha :] \quad (4)$$

which is recognized as the Hamiltonian of a free massless Dirac field and the symbols $: \dots :$ denote normal ordering with respect to the ground state of the free system.

The advantage of the linearization of the spectrum is twofold: the initial lattice problem is reformulated in terms of smooth continuum fields and – using the bosonization procedure – is mapped to the theory of two independent (in the weak-coupling limit) quantum sine-Gordon (SG) models describing charge and spin degrees of freedom, respectively.

In terms of the continuum fields the initial lattice operators have the form:

$$\begin{aligned} \hat{\rho}_{n,\alpha} - \frac{1}{2} &= a_0 \{ (J_{R,\alpha} + J_{L,\alpha}) \\ &+ (-1)^n (R_\alpha^\dagger(x) L_\alpha(x) + L_\alpha^\dagger(x) R_\alpha(x)) \}, \end{aligned} \quad (5)$$

here $J_{R,\alpha} \equiv : R_\alpha^\dagger(x) R_\alpha(x) :$ and $J_{L,\alpha} \equiv : L_\alpha^\dagger(x) L_\alpha(x) :$,

$$\vec{\mathbf{S}}(n) = a_0 \cdot \{ \vec{\mathbf{M}}(x) + (-1)^n \vec{\mathbf{L}}(x) \}. \quad (6)$$

where

$$\vec{\mathbf{M}}(x) = R_\alpha^\dagger(x) \frac{\vec{\sigma}_{\alpha\beta}}{2} R_\beta(x) + L_\alpha^\dagger(x) \frac{\vec{\sigma}_{\alpha\beta}}{2} L_\beta(x) \quad (7)$$

determines the smooth part of the spin density in the continuum limit, and

$$\vec{\mathbf{L}}(x) = R_\alpha^\dagger(x) \frac{\vec{\sigma}_{\alpha\beta}}{2} L_\beta(x) + L_\alpha^\dagger(x) \frac{\vec{\sigma}_{\alpha\beta}}{2} R_\beta(x) \quad (8)$$

is the staggered part of the local spin density.

The second step is to use the standard bosonization expressions for fermionic bilinears [28]:

$$\begin{aligned} -i \sum_\alpha [: R_\alpha^\dagger \partial_x R_\alpha : - : L_\alpha^\dagger \partial_x L_\alpha :] \rightarrow \\ \frac{1}{2} \{ (\partial_x \theta_c)^2 + (\partial_x \phi_c)^2 \} + \frac{1}{2} \{ (\partial_x \theta_s)^2 + (\partial_x \phi_s)^2 \}, \end{aligned} \quad (9)$$

$$J_{R,\alpha} + J_{L,\alpha} \rightarrow \frac{1}{\sqrt{2\pi}} [(\partial_x \phi_c) + \alpha (\partial_x \phi_s)], \quad (10)$$

$$J_{R,\alpha} - J_{L,\alpha} \rightarrow \frac{1}{\sqrt{2\pi}} [(\partial_x \theta_s) + \alpha (\partial_x \theta_s)] \quad (11)$$

$$R_\alpha^\dagger(x) R_{-\alpha}(x) \rightarrow \frac{1}{2\pi a_0} \exp(-i\alpha\sqrt{2\pi}(\phi_s - \theta_s)) \quad (12)$$

$$L_\alpha^\dagger(x) L_{-\alpha}(x) \rightarrow \frac{1}{2\pi a_0} \exp(+i\alpha\sqrt{2\pi}(\phi_s + \theta_s)) \quad (13)$$

$$R_\alpha^\dagger(x) L_\alpha(x) \rightarrow \frac{-i}{2\pi a_0} \exp(+i\sqrt{2\pi}(\phi_c + \alpha\phi_s)), \quad (14)$$

$$R_\alpha^\dagger(x) L_{-\alpha}(x) \rightarrow \frac{1}{2\pi a_0} \exp(-i\sqrt{2\pi}(\phi_c - \alpha\theta_s)). \quad (15)$$

Here scalar fields $\phi_{c,s}(x)$ describe the charge and the spin degrees of freedom and fields $\theta_{c,s}(x)$ are their dual counterparts: $\partial_x \theta_{c,s} = \Pi_{c,s}$ where $\Pi_{c,s}$ is the momentum conjugated to the field $\phi_{c,s}$.

Using bosonization formulas (9)-(15), after rescaling of the fields and lengths, the continuum-limit version of the Hamiltonian (1) acquires the following form

$$\mathcal{H} = \mathcal{H}_c + \mathcal{H}_s \quad (16)$$

where

$$\begin{aligned} \mathcal{H}_c &= v_c \int dx \left\{ \frac{1}{2} [(\partial_x \varphi_c)^2 + (\partial_x \vartheta_c)^2] \right. \\ &\quad \left. + \frac{m_c}{a_0^2} \cos(\sqrt{8\pi K_c} \varphi_c) \right\}, \end{aligned} \quad (17)$$

$$\begin{aligned} \mathcal{H}_s &= v_s \int dx \left\{ \frac{1}{2} [(\partial_x \vartheta_s)^2 + (\partial_x \varphi_s)^2] \right. \\ &\quad \left. + \frac{m_s}{a_0^2} \cos(\sqrt{8\pi K_s} \varphi_s) \right\}. \end{aligned} \quad (18)$$

Here we have defined

$$K_c \simeq 1 + \frac{1}{2} g_c, \quad m_c = -\frac{1}{2\pi} g_u, \quad (19)$$

$$K_s \simeq 1 + \frac{1}{2} g_s, \quad m_s = \frac{1}{2\pi} g_\perp, \quad (20)$$

$v_{c(s)} = v_F K_{c(s)}^{-1}$ and small dimensionless coupling constants given by:

$$g_c = g_u = -\frac{1}{2\pi t} (U + J_\perp + \frac{1}{2} J_\parallel), \quad (21)$$

$$g_s = \frac{1}{2\pi t} (U + J_\perp - \frac{3}{2} J_\parallel), \quad (22)$$

$$g_\perp = \frac{1}{2\pi t} (U - J_\perp + \frac{1}{2} J_\parallel). \quad (23)$$

The relation between K_c (K_s), m_c (m_s), and g_c (g_s), g_u (g_\perp) is universal in the weak coupling limit. In obtaining (16), several terms corresponding to scattering processes in the vicinity of a Fermi point, which lead to a renormalization of the Fermi velocities in second order in g , as well as strongly irrelevant terms $\sim \cos(\sqrt{8\pi K_c} \varphi_c) \cos(\sqrt{8\pi K_s} \varphi_s)$ describing umklapp processes with parallel spins, were omitted.

The mapping of the initial lattice Hamiltonian Eq. (1) into the continuum theory of two decoupled quantum SG models Eqs. (17)-(18) performed above allows the study the ground state phase diagram of the system based on

the infrared properties of the SG Hamiltonians. The corresponding behavior of the SG model is described by pairs of renormalization group equations for the effective coupling constants Γ_i [30]

$$d\Gamma_u/dL = -\Gamma_c\Gamma_u, \quad d\Gamma_c/dL = -\Gamma_u^2, \quad (24)$$

$$d\Gamma_\perp/dL = -\Gamma_s\Gamma_\perp, \quad d\Gamma_s/dL = -\Gamma_\perp^2, \quad (25)$$

where $L = \log(a/a_0)$ and $\Gamma_i(0) = g_i$. Each pair of equations (24) and (25) describes a Kosterlitz–Thouless transition [31] in the charge and spin channels. The flow diagram is given in Fig. 1. The flow lines lie on the hyperbola

$$\Gamma_{c(s)}^2 - \Gamma_{u(\perp)}^2 = \mu_{c(s)} = g_{c(s)}^2 - g_{u(\perp)}^2, \quad (26)$$

and – depending on the relation between the bare coupling constants $g_{c(s)}$ and $g_{u(\perp)}$ – exhibit two different regimes:

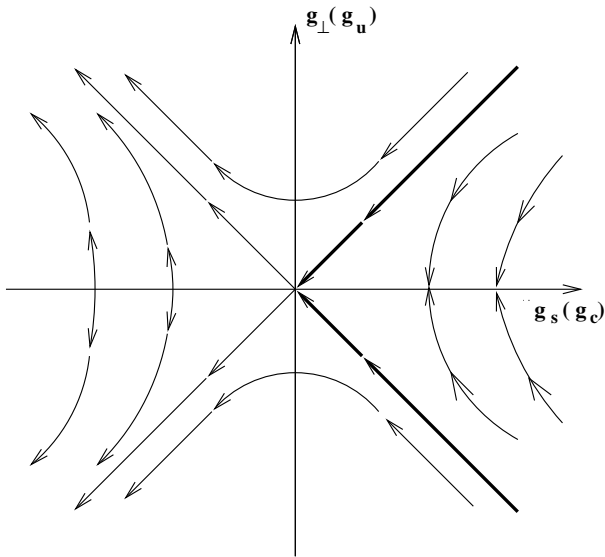


FIG. 4. The renormalization-group flow diagram; the arrows denote the direction of flow with increasing length scale.

For $g_c \geq |g_u|$ ($g_s \geq |g_\perp|$) we are in the weak coupling regime; the effective mass $M_{c(s)}$ scales to 0. The low energy (large distance) behavior of the gapless charge (spin) degrees of freedom is described by a free scalar field

$$\mathcal{H}_{c(s)} = \frac{1}{2}v_{c(s)} \int dx \{(\partial_x \theta_{c(s)})^2 + (\partial_x \varphi_{c(s)})^2\} \quad (27)$$

where $\partial_x \theta_{c(s)} = P_{c(s)}$.

The corresponding correlations show a power law decay

$$\langle e^{i\sqrt{2\pi K}\varphi(x)} e^{-i\sqrt{2\pi K}\varphi(x')} \rangle \sim |x - x'|^{-K}, \quad (28)$$

$$\langle e^{i\sqrt{2\pi/K}\theta(x)} e^{-i\sqrt{2\pi/K}\theta(x')} \rangle \sim |x - x'|^{-1/K}, \quad (29)$$

and the only parameter controlling the infrared behavior in the gapless regime is the fixed-point value of the effective coupling constants $K_{c(s)}$.

For $g_c < |g_u|$ ($g_s < |g_\perp|$) the system scales to the strong coupling regime; depending on the sign of the bare mass $m_{c(s)}$ the effective mass $M_{c(s)}$ scales to $\pm\infty$, which signals the crossover to the strong coupling regime and indicates the dynamical generation of a commensurability gap in the charge (spin) excitation spectrum. The fields φ_c (φ_s) get ordered with the vacuum expectation values [32]

$$\langle \varphi_{c(s)} \rangle = \begin{cases} \sqrt{\pi/8K_s} & (m_{c(s)} > 0) \\ 0 & (m_{c(s)} < 0) \end{cases}. \quad (30)$$

Using the initial values of the coupling constants, given in (21)-(23), we see that flow trajectories in the charge sector (due to the $SU(2)$ -charge symmetry) are along the separatrix $g_c = g_u$. Therefore, at

$$U + J_\perp + \frac{1}{2}J_\parallel > 0. \quad (31)$$

there is a gap in the charge excitation spectrum ($\Delta_c \neq 0$) and the charge field φ_c is ordered with the vacuum expectation value

$$\langle \varphi_c \rangle = 0, \quad (32)$$

while at $U + J_\perp + \frac{1}{2}J_\parallel < 0$ the charge sector is gapless and the fixed-point value of the parameter K_c^* is 1.

The $U(1)$ symmetry of the spin channel ensures more alternatives. Depending on the relation between the bare coupling constants there are **two different strong-coupling sectors in the spin channel**. For

$$U < \frac{1}{2}J_\parallel < J_\perp - U \quad (33)$$

the spin channel is massive ($\Delta_s \neq 0$) and the field φ_s gets ordered with the vacuum expectation value

$$\langle \varphi_s \rangle = 0, \quad (34)$$

while for

$$J_\perp < \min\{U + \frac{1}{2}J_\parallel; J_\parallel\} \quad (35)$$

the spin channel is massive ($\Delta_s \neq 0$), with the vacuum expectation value

$$\langle \varphi_s \rangle = \sqrt{\pi/8K_s}. \quad (36)$$

In all other cases the excitation spectrum in the corresponding channel is gapless. The low-energy behavior of the system is controlled by the fixed-point value of the Luttinger-liquid parameter $K_s^* = 1 + \frac{1}{2}g_s^*$.

However, in the particular case of strong antiferromagnetic easy-plane anisotropy ($J_\perp \gg |J_\parallel|$), the clarification of details of the phase diagram requires a closer inspection. Let us first consider the XY limit of the model: $U = J_\parallel = 0$. As we see, the initial values of the coupling constants g_s and g_\perp , given in (22)-(23), lie exactly on the

separatrix $g_s = -g_\perp$ and scale to the $SU(2)$ -symmetric fixed-point value $g_s = g_\perp = 0$. However, due to the low $U(1)$ -symmetry of the model, there is no symmetry reason which would guarantee that the bare couplings lie *exactly* on the separatrix. As we will show below, the higher order (finite band) effects push the scaling trajectories from the separatrix. For details of the method we refer the reader to the paper [33] where a similar effect in the pair-hopping model was considered.

Since in first order the couplings lie on the separatrix, we must work to $O(J^2)$. We find, that in the $SU(2)$ -symmetric case ($J_\perp = J_\parallel = J$) $g_s - |g_\perp| = 0$ up to $O(J^2)$, but for $J_\perp \neq J_\parallel$ there is an $O((J_\perp - J_\parallel)^2)$ correction to this quantity. This correction occurs due to the nonlocal character of the interaction and to deviations from the linear dispersion relations for electrons on the lattice.

In particular, upon integrating out all modes with momenta outside the small region around each Fermi point $|p - p_F| < \Lambda \equiv 2/a$, where Λ is small compared to p_F , we obtain the effective theory described by equations (17)-(18), with the following coupling constants:

$$g_c = g_u = -\frac{1}{2\pi t}(J_\perp + \frac{1}{2}J_\parallel) + \frac{1}{(2\pi t)^2} \left(J_\perp J_\parallel - \frac{1}{4}J_\parallel^2 \right) - \frac{1}{(2\pi t)^2} \left(J_\perp + \frac{1}{2}J_\parallel \right)^2 \log(a/a_0), \quad (37)$$

$$g_\perp = \frac{1}{2\pi t} \left(\frac{1}{2}J_\parallel - J_\perp \right) - \frac{1}{(2\pi t)^2} \left(J_\perp^2 - 2J_\perp J_\parallel + \frac{1}{4}J_\parallel^2 \right) - \frac{1}{(2\pi t)^2} \left(J_\perp - \frac{3}{2}J_\parallel \right) \left(\frac{1}{2}J_\parallel - J_\perp \right) \log(a/a_0) \quad (38)$$

$$g_s = \frac{1}{2\pi t} \left(J_\perp - \frac{3}{2}J_\parallel \right) + \frac{1}{(2\pi t)^2} \left(2J_\perp^2 - J_\perp J_\parallel - \frac{1}{2}J_\parallel^2 \right) - \frac{1}{(2\pi t)^2} \left(J_\perp - \frac{1}{2}J_\parallel \right)^2 \log(a/a_0). \quad (39)$$

Thus we see, while the bare couplings g_c and g_u always lie on the $SU(2)$ separatrix, g_s equals $|g_\perp|$ only in the $SU(2)$ -symmetric case $J_\perp = J_\parallel = J$:

$$g_s = g_\perp = -\frac{J}{4\pi t} - \frac{J^2}{4(2\pi t)^2} [\log(a/a_0) - 3]. \quad (40)$$

In the case of the XY model the corresponding parameters are:

$$g_\perp = -\frac{1}{2\pi t}J_\perp + \frac{1}{(2\pi t)^2}J_\perp^2 [\log(a/a_0) - 1] \quad (41)$$

$$g_s = \frac{1}{2\pi t}J_\perp - \frac{1}{(2\pi t)^2}J_\perp^2 [\log(a/a_0) - 2]. \quad (42)$$

Thus we see that the values of the coupling constants g_\perp and g_s move off the separatrix into the region of the flow diagram that flows to non-zero g_s . This movement occurs because now

$$\mu = g_s^2 - g_\perp^2 = (J_\perp/2\pi t)^3 + O(J_\perp/t)^4 > 0. \quad (43)$$

To actually find the end-point value of the parameter Γ_s , we need the second order renormalization group equations for the effective coupling constants. These equations read [34]

$$d\Gamma_\perp/dL = -\Gamma_s\Gamma_\perp - \frac{1}{2}\Gamma_\perp^3, \\ d\Gamma_s/dL = -\Gamma_\perp^2 - \frac{1}{2}\Gamma_\perp^2\Gamma_s. \quad (44)$$

Combing equations (44)-(43) one obtains

$$d\mu/dL = -\Gamma_\perp^2\mu. \quad (45)$$

Substituting the first-order solution for Γ_\perp and solving (45) we obtain

$$\mu(\infty) \equiv (g_s^*)^2 = \left(\frac{J_\perp}{2\pi t} \right)^3 \exp(-J_\perp/2\pi t). \quad (46)$$

At small $J_\perp > 0$ the XY model scales to a point on the fixed-point line $\Gamma_\perp = 0$ which approaches the $SU(2)$ end-point at $J_\perp \rightarrow 0$ and moves along the critical line with increasing parameter J_\perp .

Using (39) and (38) and applying a similar analysis in the case $J_\parallel \neq 0$, one easily obtains that a gapless regime in the spin channel exists for

$$J_\perp \leq \sqrt{2\pi t J_\parallel}. \quad (47)$$

III. THE WEAK-COUPLING PHASE DIAGRAM

Let us now consider the weak-coupling ground state phase diagram of the model Eq. (1).

A. Order parameters

To clarify the symmetry properties of the ground states of the system in different sectors of the phase diagram we use the following set of order parameters describing the short wave-length fluctuations of the *site-located* charge density,

$$\Delta_{CDW} = (-1)^n \sum_\alpha c_{n,\alpha}^\dagger c_{n,\alpha} \\ \sim \sin(\sqrt{2\pi K_c} \varphi_c) \cos(\sqrt{2\pi K_s} \varphi_s), \quad (48)$$

the *site-located* spin density,

$$\Delta_{SDW^z} = (-1)^n \sum_\alpha \alpha c_{n,\alpha}^\dagger c_{n,\alpha} \\ \sim \cos(\sqrt{2\pi K_c} \varphi_c) \sin(\sqrt{2\pi K_s} \varphi_s) \quad (49)$$

$$\Delta_{SDW^x} = (-1)^n \sum_\alpha c_{n,\alpha}^\dagger c_{n,-\alpha}$$

$$\sim \cos(\sqrt{2\pi K_c \varphi_c}) \cos(\sqrt{\frac{2\pi}{K_s} \theta_s}), \quad (50)$$

$$\begin{aligned} \Delta_{SDW^y} &= i(-1)^n \sum_{\alpha} \alpha c_{n,\alpha}^{\dagger} c_{n,-\alpha} \\ &\sim \cos(\sqrt{2\pi K_c \varphi_c}) \sin(\sqrt{\frac{2\pi}{K_s} \theta_s}), \end{aligned} \quad (51)$$

and the short wave-length fluctuations of the *bond-located* charge density,

$$\begin{aligned} \Delta_{dimer} &= (-1)^n \sum_{\alpha} (c_{n,\alpha}^{\dagger} c_{n+1,\alpha} + H.c.) \\ &\sim \cos(\sqrt{2\pi K_c \varphi_c}) \cos(\sqrt{2\pi K_s \varphi_s}). \end{aligned} \quad (52)$$

In addition we use two superconducting order parameters corresponding to singlet (Δ_{SS}) and triplet (Δ_{TS}) superconductivity:

$$\begin{aligned} \Delta_{SS}(x) &= R_{\uparrow}^{\dagger}(x) L_{\downarrow}^{\dagger}(x) - R_{\downarrow}^{\dagger}(x) L_{\uparrow}^{\dagger}(x) \\ &\sim \exp(i\sqrt{\frac{2\pi}{K_c} \theta_c}) \cos(\sqrt{2\pi K_s \varphi_s}), \end{aligned} \quad (53)$$

$$\begin{aligned} \Delta_{TS}(x) &= R_{\uparrow}^{\dagger}(x) L_{\downarrow}^{\dagger}(x) + R_{\downarrow}^{\dagger}(x) L_{\uparrow}^{\dagger}(x) \\ &\sim \exp(i\sqrt{\frac{2\pi}{K_c} \theta_c}) \sin(\sqrt{2\pi K_s \varphi_s}). \end{aligned} \quad (54)$$

B. Phases

With the results of the previous section for the excitation spectrum and the behavior of the corresponding fields Eqs. (28)–(30) we now analyze the ground state phase diagram of the model (1) (see Fig. 5 and Fig. 6).

Let us first consider the sector of the phase diagram corresponding to $U + J_{\perp} + \frac{1}{2}J_{\parallel} > 0$, characterized by a **gap in the charge excitation spectrum**. In this case we obtain the following regimes of behavior:

- **A.** $\Delta_c \neq 0, \Delta_s \neq 0, \langle \varphi_c \rangle = \langle \varphi_s \rangle = 0$;

This regime corresponds to the appearance of a long-range ordered *dimerized (Peierls)* phase

$$\langle \Delta_{dimer}(x) \Delta_{dimer}(x') \rangle \sim \text{constant} \quad (55)$$

in the ground state of the model. This phase is realized in the case of *dominating antiferromagnetic exchange*, in particular for isotropic exchange $J_{\parallel} = J_{\perp} = J > 2U$.

- **B.** $\Delta_c \neq 0, \Delta_s \neq 0, \langle \varphi_c \rangle = 0, \langle \varphi_s \rangle = \sqrt{\pi/8K_s}$;

This regime corresponds to the appearance of a long-range ordered *antiferromagnetic (Neel)* phase

$$\langle \Delta_{SDW^z}(x) \Delta_{SDW^z}(x') \rangle \sim \text{constant} \quad (56)$$

in the ground state. In this regime the Hubbard model is extended by incorporating an easy-axis spin exchange interaction.

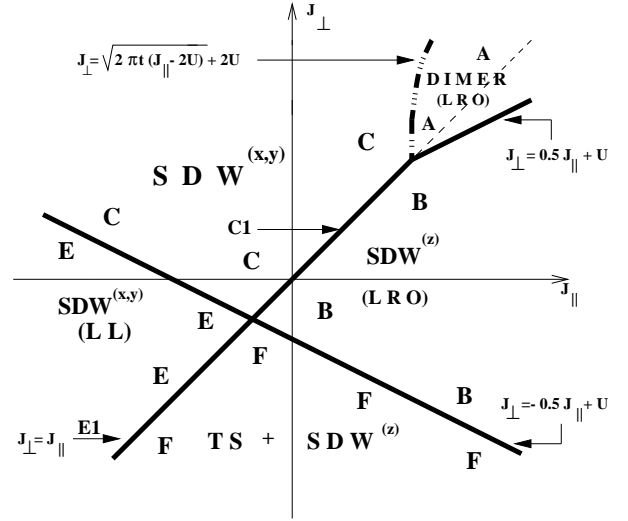


FIG. 5. The weak-coupling phase diagram of the model (1) at $U > 0$

- **C.** $\Delta_c \neq 0, \langle \varphi_c \rangle = 0, \Delta_s = 0$;

The charge excitation spectrum is gapped. Ordering of the field φ_c with vacuum expectation value $\langle \varphi_c \rangle = 0$ leads to a suppression of the *CDW* and *superconducting* correlations. The *SDW* and *Peierls* correlations show a power-law decay at large distances. The low-energy properties of the gapless spin degrees of freedom are controlled by the fixed-point value of the Luttinger liquid parameter K_s^* .

In the $SU(2)$ -spin symmetric case

- **C1.** $J_{\parallel} = J_{\perp} = J, \quad -\frac{2}{3}U < J < 2U$;

$K_s^* = 1$ and the *Peierls* and SDW^i ($i = x, y, z$) correlations show *identical power-law decay* at large distances:

$$\begin{aligned} \langle \Delta_{dimer}(x) \Delta_{dimer}(x') \rangle &\simeq \langle \Delta_{SDW}(x) \Delta_{SDW}(x') \rangle \\ &\sim |x - x'|^{-1}. \end{aligned} \quad (57)$$

In the general case of $U(1)$ -spin symmetry, $K_s^* > 1$ and the “*in-plane*” $SDW^{x,y}$ correlations dominate in the ground state,

$$\begin{aligned} \langle \Delta_{SDW^x}(x) \Delta_{SDW^x}(x') \rangle &\simeq \langle \Delta_{SDW^y}(x) \Delta_{SDW^y}(x') \rangle \\ &\sim |x - x'|^{-1/K_s^*}, \end{aligned} \quad (58)$$

while the *Peierls* and SDW^z correlations decay faster,

$$\begin{aligned} \langle \Delta_{dimer}(x) \Delta_{dimer}(x') \rangle &\simeq \langle \Delta_{SDW}(x) \Delta_{SDW}(x') \rangle \\ &\sim |x - x'|^{-K_s^*}. \end{aligned} \quad (59)$$

This case corresponds to an extension of the Hubbard model by incorporating an easy-plane spin exchange interaction.

Let us now consider the sector $U + J_{\perp} + \frac{1}{2}J_{\parallel} < 0$ in which the charge excitation spectrum is gapless.

The following different regimes are realized in this sector:

- **D.** $\Delta_c = 0, \Delta_s \neq 0, \langle \varphi_s \rangle = 0$;

This phase is realized in the case of *dominating attractive Hubbard interaction*, in particular for isotropic exchange $J_{\parallel} = J_{\perp} = J$ at $2U < J < -\frac{2}{3}U$.

There is a gap in the spin excitation spectrum. The spin field is ordered, $\langle \varphi_s \rangle = 0$. Ordering of the field $\langle \varphi_s \rangle$ leads to a *suppression* of the *SDW* and *TS* fluctuations. The low-energy properties of the gapless charge degrees of freedom are controlled by the fixed-point value of the Luttinger liquid parameter K_c^* .

In the case of a half-filled band which we are considering here the charge degrees of freedom are governed by the $SU(2)$ -charge symmetry. The fixed-point value of the parameter K_c (due to the $SU(2)$ -charge symmetry) is $K_c^* = 1$. The *CDW*, *SS*, and *Peierls* correlations show identical power-law decay at large distances,

$$\begin{aligned} \langle \Delta_{CDW}(x)\Delta_{CDW}(x') \rangle &= \langle \Delta_{SS}(x)\Delta_{SS}(x') \rangle = \\ \langle \Delta_{dimer}(x)\Delta_{dimer}(x') \rangle &\sim |x - x'|^{-1}. \end{aligned} \quad (60)$$

- **E.** $\Delta_c = 0, \Delta_s = 0$;

In this case the Luttinger liquid (*LL*) phase is realized.

The charge and the spin channel are gapless. the low-energy behavior of the system is controlled by the Luttinger liquid parameters K_c^* and K_s^* .

In the case of $SU(2)$ -invariant spin exchange

- **E1.** $J_{\parallel} = J_{\perp} = J < \min\{-\frac{2}{3}U, 2U\}$

$K_c^* = K_s^* = 1$ and all correlations show $|x - x'|^{-2}$ decay at large distances.

In the case of a $U(1)$ -symmetric spin channel, the *LL* phase is realized for easy-axis ferromagnetic anisotropy. In this case $K_c^* = 1, K_s^* > 1$ and in the weak-coupling limit the in-plane antiferromagnetic correlations dominate

$$\langle \Delta_{SDW^{x,y}}(x)\Delta_{SDW^{x,y}}(x') \rangle \sim |x - x'|^{-1-1/K_s}. \quad (61)$$

- **F.** $\Delta_c = 0, \Delta_s \neq 0, \langle \varphi_s \rangle = \sqrt{\pi/8K_s}$;

This sector of the phase diagram is dual to the sector **D**. As common in the half-filled band case, the gapless charge excitation spectrum opens a possibility for the realization of a *superconducting* instability in the system. Moreover, due to the $U(1)$ -symmetry of the system, ordering of the φ_s with vacuum expectation value $\langle \varphi_s \rangle = \sqrt{\pi/8K_s}$ leads to a suppression of the *CDW* and *SS* correlations. In this case the *SDW* and *TS* fluctuations show identical power-law decay at large distances,

$$\begin{aligned} \langle \Delta_{SDW}(x)\Delta_{SDW}(x') \rangle &= \langle \Delta_{TS}(x)\Delta_{TS}(x') \rangle \\ &\sim |x - x'|^{-1}, \end{aligned} \quad (62)$$

and are the *dominating instabilities* in the system. This phase is realized only for anisotropic spin exchange in the case of strong *ferromagnetic easy-plane* anisotropy.

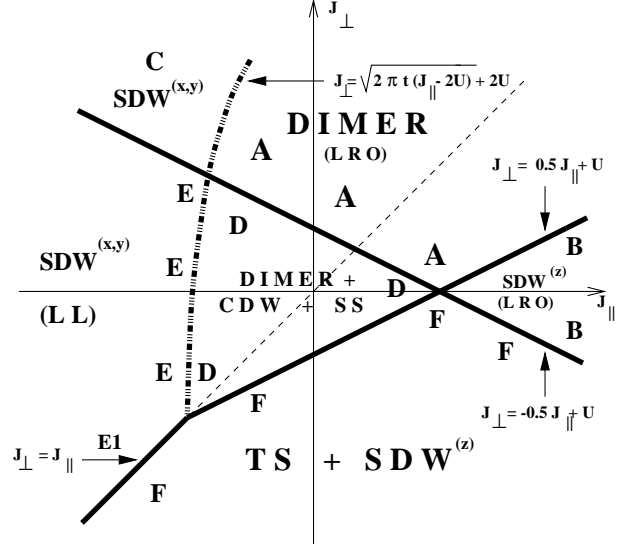


FIG. 6. The weak-coupling phase diagram of the model (1) at $U < 0$

IV. DISCUSSION AND SUMMARY

In this paper we have studied the one-dimensional $t-J$ model of correlated electrons in the case of a half-filled band. This model describes a system of itinerant electrons with spin-exchange interaction between electrons on nearest-neighbor sites. We have demonstrated that in the case of easy-plane anisotropic ferromagnetic exchange the *triplet superconducting* and *SDW* instabilities are the dominating instabilities in the system. These instabilities remain dominating instabilities in the ground state also for moderate values of the on-site Hubbard interaction. We stress that, in 1D this phase can be realized only in the case of $U(1)$ -spin symmetry. This result is in agreement with recent experimental results showing strong easy-plane anisotropy of ferromagnetic spin fluctuations in the triplet superconductor Sr_2RuO_4 [10]. We want to stress, that although in this paper we presented results considering the half-filled band case only, it is obvious that doping will split the degeneracy between the *TS* and *SDW* phases and will favor the superconducting instability in the system.

We also demonstrated a strong enhancement of tendencies towards Peierls ordering in the electron system caused by an isotropic (or weakly anisotropic) antiferromagnetic exchange. We have shown that the half-filled

$t-J$ model shows a long-range dimerized (Peierls) ordering in the ground state in the case of antiferromagnetic exchange.

We also demonstrated the importance of the finite-band effects in this model and presented a qualitative description of the transition from the band-dominated $TS+SDW$ phase into the insulating spin-1/2 magnetic XY phase. Detailed numerical studies of the phase diagram for strong exchange coupling and for arbitrary filling are in progress and will be published elsewhere.

ACKNOWLEDGMENTS

GJ acknowledges helpful discussions with D. Baeriswyl, C. Dziurzik, A.P. Kampf, A.A. Nersesyan and A. Schadschneider. This work was supported by the Deutsche Forschungsgemeinschaft in the framework of the research program of the Sonderforschungsbereich 341. GJ acknowledges INTAS support under the Grant GEORGIA-INTAS No. 97-1340.

¹ Permanent Address: Institute of Physics, Georgian Academy, Tamarashvili 6, Tbilisi 380077, Georgia. Electronic address: japa@iph.hepi.edu.ge

- [1] Y. Maeno, H. Hashimoto, K. Yoshida, S. Nishizaki, T. Fujita, J.G. Berdnorz, and F. Lichtenberg, *Nature* **372**, 532 (1994).
- [2] A.P. Mackenzie, S.R. Julian, A.J. Diver, G.G. Lonzarich, Y. Maeno, S. Nishizaki, and T. Fujita, *Phys. Rev. Lett.* **80**, 161 (1998).
- [3] K. Ishida, Y. Kitaoka, K. Asayama, S. Ikeda, S. Nishizaki, Y. Maeno, K. Yoshida, and T. Fujita, *Phys. Rev. B* **56**, R505 (1997).
- [4] G.M. Luke, Y. Fudamoto, K.M. Kojima, M.I. Larkin, J. Merrin, B. Nachumi, Y.J. Uemura, Y. Maeno, Z.Q. Mao, Y. Mori, H. Nakamura, and M.Sigrist, *Nature* **394**, 558 (1998).
- [5] T.M. Rice and M.Sigrist, *J. of Phys., Condens. Matter* **7**, L643 (1995).
- [6] G. Baskaran, *Physica B* **223-224**, 490 (1996).
- [7] K. Machida, M. Ozaki, and T. Ohmi, *J. Phys. Soc. Jpn.* **65**, 3720 (1996).
- [8] M.Sigrist, D. Agterberg, A. Furusaki, C. Honercampf, K.K. Ng, T.M. Rice, and M.E. Zhitomirsky, *cond-mat/9902214*.
- [9] T. Imai, A.W. Hunt, K.R. Thurber, and F.C. Chou, *Phys. Rev. Lett.* **81**, 3006 (1998).
- [10] H. Mukuda, K. Ishida, Y. Kitaoka, K. Asayama, Z.Q. Mao, Y. Mori, and Y. Maeno, *Physica B* **259-261**, 944 (1999).
- [11] I.I. Mazin and D.J. Singh, *Phys. Rev. Lett.* **79**, 733 (1997).
- [12] D. Jerome, A. Mazaud, M. Ribault, and K. Bechgaard, *J. Phys. (Paris) Lett.* **41**, L92 (1980).
- [13] D. Jerome, *Science* **252**, 1509 (1991).
- [14] A.A. Abrikosov, *J. Low Temp. Phys.* **53**, 359 (1983); L.P. Gor'kov and D. Jerome, *J. Phys. (Paris) Lett.* **46**, L643 (1985).
- [15] M.Y. Choi, P.M. Chaikin, and R.L. Green, *Phys. Rev. B* **25**, 6208 (1982); S. Tomic et al., *J. Phys. (Paris) Colloq.* **44**, C3-1075 (1983); C. Coulon et al., *J. Phys. (Paris)* **43**, 1723 (1983).
- [16] M. Takigawa, H. Yosuoka and G. Saito, *J. Phys. Soc. Jpn.* **56**, 873 (1987); I.J. Lee, M.J. Naughton, G.M. Danner, and P.M. Chaikin, *Phys. Rev. Lett.* **78**, 3555 (1997); S. Belin and K. Behnia, *Phys. Rev. Lett.* **79**, 2125 (1997).
- [17] E. Dagotto, J. Riera, and D.J. Scalapino, *Phys. Rev. B* **45**, 5744 (1992).
- [18] T.M. Rice, M. Troyer, and H. Tsunetsugu, *J. Phys. Chem. Solids* **56**, 1663 (1995).
- [19] R. Arita, K. Kuroki, H. Aoki, and M. Fabrizio, *cond-mat/9712134*
- [20] S. Daul, D.J. Scalapino, and S. White, *cond-mat/9907301*
- [21] J. Solyom, *Adv. Phys.* **28**, 201 (1979).
- [22] Y. Hasegawa and H. Fukuyama, *J. Phys. Soc. Jpn.* **55**, 3978, (1986); *ibid.*, **56**, 877 (1987).
- [23] V.J. Emery, in *Highly Conducting One-Dimensional Solids*, edited by J.T. Devreese, R.P. Evrard, and V.E. Van Doren, Plenum, New York (1979).
- [24] J. Voit, *Phys. Rev. B* **45**, 4027 (1992).
- [25] H. Frahm and V.E. Korepin, *Phys. Rev. B* **42**, 10553 (1990); N. Kawakami and S.-K. Yang, *Phys. Lett. A* **148**, 359 (1990).
- [26] Here we use the analogy between the itinerant- XY and the pair-hopping model. The one spin component electron-hole transformation $c_{n,\uparrow} \rightarrow c_{n,\uparrow}, c_{n,\downarrow} \rightarrow (-1)^n c_{n,\downarrow}^\dagger$ interchanges the charge and spin degrees of freedom, and maps the transverse exchange part into the pair-hopping coupling $\frac{1}{2}J_\perp(S_n^+ S_{n+1}^- + h.c.) \rightarrow -\frac{1}{2}J_\perp(c_{n,\uparrow}^\dagger c_{n,\downarrow}^\dagger c_{n+1,\downarrow} c_{n+1,\uparrow} + h.c.)$. In the case of a half-filled band a transition from the insulating into an η -superconducting phase takes place at $-\frac{1}{2}J_\perp \sim 2t$ in the pair-hopping model. This transition is first order (level crossing) and at the transition the charge gap closes and a spin gap opens [27].
- [27] A. Sikkema and I. Affleck, *Phys. Rev. B*, **52**, 10207 (1995); G. Bouzerar and G.I. Japaridze, *Zeit. Phys. B*, **104**, 215 (1997).
- [28] For a recent review see A.O. Gogolin, A.A. Nersesyan and A.M. Tsvelik, *Bosonization and strongly correlated systems*, Cambridge University Press (1998).
- [29] A. Luther and V.J. Emery, *Phys. Rev. Lett.* **33**, 589 (1974).
- [30] P. Wiegmann, *J. Phys. C* **11**, 1583 (1978)
- [31] J.M. Kosterlitz and D. Thouless, *J. Phys. C: Solid State Phys.* **6**, 1181 (1973); *ibid.* **7**, 1046 (1974).
- [32] K.A. Muttalib and V.J. Emery, *Phys. Rev. Lett.* **57**, 1370 (1986); T. Giamarchi and H.J. Schulz, *Jour. Phys. (Paris)* **49**, 819 (1988); *Phys. Rev. B* **33**, 2066 (1988).
- [33] I. Affleck and J.B. Marston, *J. Phys. C* **21**, 2511 (1988).
- [34] D. Amit and B. Grinstein, *J. Phys. A* **13**, 585 (1980); D.

Boyanovsky, J. Phys. A **22**, 2601 (1989).